

Model-based energy efficient global path planning for a four-wheeled mobile robot

by

Piotr Jaroszek and Maciej Trojnecki

Industrial Research Institute for Automation and Measurements PIAP,  
Al. Jerozolimskie 202, 02-486 Warsaw, Poland  
pjaroszek@piap.pl, mtrojnecki@piap.pl

**Abstract:** This paper concerns an energy efficient global path planning algorithm for a four-wheeled mobile robot (4WMR). First, the appropriate graph search methods for robot path planning are described. The A\* heuristic algorithm is chosen to find an optimal path on a 2D tile-decomposed map. Various criteria of optimization in path planning, like mobility, distance, or energy are reviewed. The adequate terrain representation is introduced. Each cell in the map includes information about ground height and type. Tire-ground interface for every terrain type is characterized by coefficients of friction and rolling resistance. The goal of the elaborated algorithm is to find an energy minimizing route for the given environment, based on the robot dynamics, its motor characteristics, and power supply constraints. The cost is introduced as a function of electrical energy consumption of each motor and other robot devices. A simulation study was performed in order to investigate the power consumption level for diverse terrain. Two 1600 m<sup>2</sup> test maps, representing field and urban environments, were decomposed into 20x20 equal-sized square-shaped elements. Several simulation experiments have been carried out to highlight the differences between energy consumption of the classic shortest path approach, where cost function is represented as the path length, and the energy efficient planning method, where cost is related to electrical energy consumed during robot motion.

**Keywords:** four-wheeled mobile robot; global path planning; robot dynamics model; heuristic algorithm; energy efficiency

## 1. Introduction

Autonomous mobile robots need to operate in the world, where the real physical laws and limitations are present. In addition, their workspace is often populated by obstacles, which make path planning a very complex task. One of the known solutions to this problem is to use the approach based on an intelligent agent. The intelligent agent is described in Russell and Norvig (1995) as an artificial

intelligence system, whose purpose is to operate on any available data and to arrive at desirable actions for a stated problem.

One may distinguish between the local and global path planning (Bigaj, 2012). The global path planning is a process of “thinking” over a larger scale, based on the global data provided infrequently, aimed at moving between desired locations on the absolute map to reach the destination. The local path planning focuses on executing a route given by global planning methods in every time step of robot operation. It is often referred to as obstacle avoidance (Szulczyński, Pazderski and Kozłowski, 2011; McNinch, Muske, Ashrafiuon, Peyton and Soltan, 2011) where the obstacle might be unknown at the previous stage of global planning and/or might be in motion. Because of this connection between both methods, global and local path planning are often paired together for complex navigation purposes. However, in this paper the random local obstacles and their avoidance is not taken into account.

The key issue in the field of autonomous mobile robotics is to find the optimal path according to certain chosen criteria. Optimization criteria depend on the problem faced and the way it is formulated. In most of studies, “the best” path implies the shortest length of the path. The problem may, however, require minimization of the corresponding travel time (Lau, Sprunk and Burgard, 2009), risk (Greytak and Hover, 2009), energy, or any other relevant factor.

Apart from the optimization of the cost function, the physical constraints, which reduce the number of possible paths, are also very important. Mobile robots usually carry with themselves a power source of limited capacity, voltage, and current. Also electric motors are constrained in terms of maximum electric power, speed, and torque. A mobile robot operating in an environment can encounter an obstacle or the changes in the type of terrain. This may result in conditions, where demand for power, torque or some other variables, associated with the motor, will rise above the level that can be provided. This, in turn, can render the path unsuitable for movement.

Terrain representation in the energy efficient planning is usually restricted to a 2D flat map decomposed into tiles with certain properties, which usually do not include terrain height. In case of exploration robots, the existing solutions are focused mainly on avoidance of repeated coverage of the same places (Mei, Lu, Hu and Lee, 2004), and as a rule they do not include terrain properties. Zheng Sun and John Reif included terrain height in addition to friction in their considerations of energy-minimizing paths (Zheng and Reif, 2003), but their work did not discuss the model of robot dynamics. More details about optimization criteria can be found in Section 4.

The motivation for the study, reported in this article was that usually the authors present the global path planning problem as the problem of finding the shortest path only. Indeed, this problem should be treated more widely, i.e., as the optimization problem in which more comprehensive criteria can be used: path length, travel time, energy consumption, etc.

## 2. The concept of the method

The objective of this paper is to solve the global path planning problem for a four-wheeled mobile robot, in which the main assumption is determination of the optimal path in terms of electric energy, based on the model of the robot and its environment.

The novelty of the presented approach consists in inclusion of several factors, which have significant impact on energy consumption and which are often omitted by other authors, i.e.:

- frictional properties of tire-ground interface for various types of terrain,
- various height of terrain in combination with the direction of motion (e.g., uphill, downhill),
- model of robot dynamics,
- consumption of electric power by robot equipment, which may be the most important factor besides the motor itself, in terms of energy usage,
- battery limitations (capacity and maximum voltage),
- cost of the robot motion on specific terrain is calculated on-line based on robot dynamics model and terrain type / slope so it is not bound, as usually, to a particular piece of terrain.

According to the knowledge of the present authors, this type of approach to the global path planning problem has not been proposed so far. None of the publications related to this problem, known to the present authors, includes all of these features.

The simulation study, performed using the proposed method of search with the A\* algorithm, shows the influence of these factors on energy consumption and on the choice of a suitable cost function for the algorithm. It also highlights cases when the described approach should be used and when it is reduced to the problem of optimization of the path length.

The assumed approach to energy efficient global path planning is described in details in subsequent sections of this work. It includes the following stages (Fig. 1):

- selection of possible new positions of a robot for further analysis, that is, the directions of search in a graph using the A\* algorithm (Section 3);
- calculation of the robot roll and pitch angles during its motion on the analyzed parts of the path on the basis of environment maps and assumed terrain representation (Section 6);
- determination of driving torques and ground reaction forces from the model of robot's dynamics (Section 5);
- checking the possibility of the robot passing through the analyzed parts of the path, for calculated roll / pitch angles, based on calculated ground reaction forces (calculated normal reaction forces should be non-negative whilst tangent reaction forces should be higher or equal to maximum friction) (Section 5);
- for the robot movement with assumed velocity (Section 5), calculation of the required current, control (input) voltage and electrical power con-

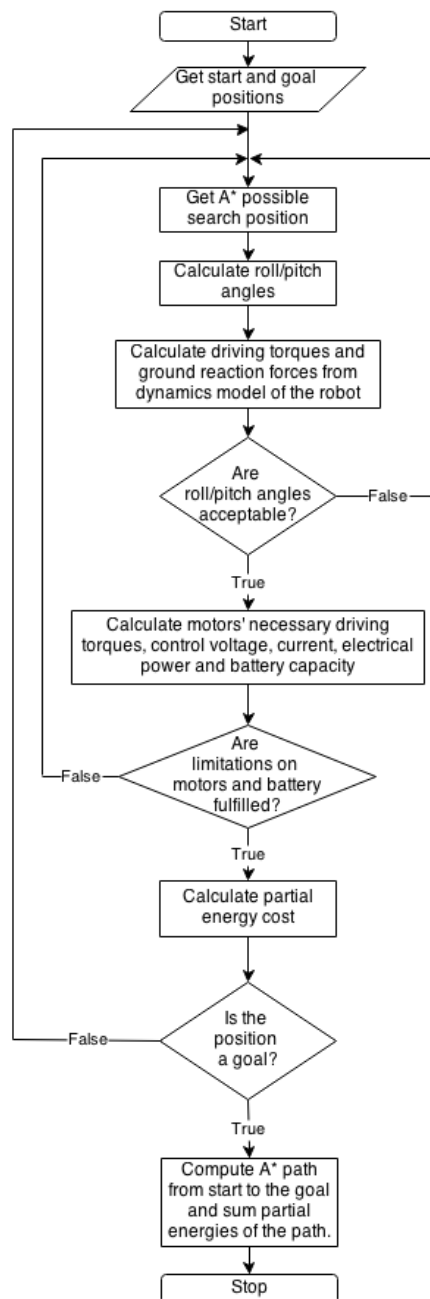


Figure 1. Flowchart of the presented global path planning algorithm

sumption from the drive model, and required battery capacity (Section 6);

- checking the constraints on maximum control voltage, current, electrical power of the drives (Section 5) as well as on maximum battery capacity (Section 6);
- determination of the partial energy cost of the robot for travelling the analyzed parts of path (Section 6)
- locally optimal choice of the direction of movement between successive nodes using the A\* algorithm based on assumed quality or optimization criterion (Section 3).

The operation of the global path planning algorithm ends when the robot reaches the specified destination, on condition that it is possible to achieve this outcome.

### 3. Pathfinding algorithms

An optimal and efficient search algorithm is essential for handling the problem of path planning. Various simplifications are considered for planning a path for mobile robots using the chosen algorithm, e.g., discontinuity of the world, deterministic behavior of actions, or constant velocity.

The global path planning task often uses search algorithms operating on the graph structure representation of the environment. Graph search algorithms can be divided into the informed, like the A\* algorithm proposed by Nilsson in 1968 (Heart, Nilsson and Bertram, 1968), which is widely used in robotics (Liu and Sun, 2011) and electronics, and the uninformed (e.g. the Dijkstra algorithm) which is also used in robotic path search (Yu, Wang and Yuan, 2011). In general, the informed search algorithms work faster than the uninformed ones, as they include additional information about the desired final robot state. If they are admissible, as this will be explained further on, they also return optimal results.

In this paper, for energy efficient path planning, a global and informed search algorithm A\* is chosen, and the graph structure is used to store the map information. The A\* algorithm, one of the most popular informed search algorithms, is complete, which means that it will always find a solution, if it exists. The A\* visits successive nodes of the graph with the lowest known cost, defined by the cost function  $f(n_i)$ , keeping the information about all the previously visited nodes in priority queue for further path search. This function is defined as follows (Heart, Nilsson and Bertram, 1968):

$$f(n_i) = g(n_i) + h(n_i), \quad (1)$$

where  $g(n_i)$  is the current path cost from the start node to node  $n_i$ , which is equal to zero at the start node;  $h(n_i)$  is a heuristic function that estimates the cost from the node  $n_i$  to the goal node. The heuristic function must be admissible if one wants the result path to have the minimum cost, that is, to be optimal.

The heuristic function is admissible if it never overestimates the real remaining cost of the potential path  $\bar{h}(n_i)$ , that means, if:

$$h(n_i) \leq \bar{h}(n_i). \quad (2)$$

The A\* algorithm generates a path  $P$ , represented by a broken line connecting the list of nodes. The robot path is denoted by  $P = \{n_0, n_1, n_2, n_3, \dots, n_K\}$ , the  $i^{th}$  node as  $n_i$ , and the partial segment of the robot path between nodes  $n_{i-1}$  and  $n_i$  as  $s_i = n_{i-1}n_i$ , where  $i = 1, 2, 3, \dots, K$ , and  $K+1$  is the total number of nodes that form the path  $P$ .

The A\* algorithm has been modified, since it was first presented, to handle dynamic map changes, into the algorithm D\* (Stentz, 1995), which then was yet modified so as to allow for any linear path from cell to cell – Field D\* (Stentz and Ferguson, 2005). Since the here presented problem is not connected with the dynamic changes in the environment, and the shape of the path, the original A\* was chosen to be the path planning algorithm.

One of the main requirements for achieving the desired energy efficient path using the A\* algorithm is to describe the energy cost function  $g(n_i)$  in an appropriate manner.

#### 4. Optimization criteria in path planning

The global heuristic cost-dependent path planning algorithms require the appropriate cost function representation in order to match the specific optimization criteria. The first term of the cost function (1), i.e.,  $g(n_i)$ , is equal to the sum of partial costs between the states of the start position  $n_0$  and the current node position  $n_i$  of the robot agent. The heuristic term  $h(n_i)$  estimates the cost of the remaining path, which has not been found yet, and which must be lower or equal to the actual cost required to move the robot from the position  $n_i$  to the goal  $n_K$ , so as to keep the algorithm admissible.

The representation of  $g(n_i)$  depends on the assumed criteria. They can include: distance, time, energy, or any other relevant factor.

##### 4.1. Path length

The most commonly used cost criterion in the path planning problem is the path length, the path with the shortest length being deemed optimal (Russell and Norvig, 1995). Cost is directly associated with the distance travelled, and the heuristic is associated with the shortest possible distance from the current node to the goal. In the environments of high uniformity, this approach can often imply other criteria, like energy consumption or travel time, because of the respective constant cost characteristics along the whole path. This means that if every partial cost associated with a partial distance travelled is the same, then the whole cost is minimal when the path consists of the minimum number of nodes. This simplification is surely too strong for most of the real life prob-

lems and cannot be used without thorough knowledge of the robot design and environment representation.

The shortest paths found by the GPS navigation systems are not the most attractive ones, because they were not calculated with any additional information about the path difficulty. This may cause further problems with executing the movement along such paths.

#### 4.2. Mobility

The different models of mobile robots sometimes impose the requirement that the specific mobility factors be also included. Steady movement is the most preferable, because of its constant energy consumption characteristic. Turns, accelerations and other maneuvers require larger forces than needed only to overcome the friction force, which implies larger energy consumption. The problem of saving energy may lead to avoidance of frequent maneuvers or to following a specific policy, e.g., in the right-hand road traffic, turning right is in most cases more attractive for a driver than turning left. In the 2008 DARPA Challenge, the Stanford team introduced in their autonomous vehicle the cost penalties for driving reverse and for changing the direction of motion (Dolgov, Thrun, Montemerlo and Diebel, 2008). More about turning-based restrictions in path planning can be found in Winter (2002). Note that these costs cannot be stored as attributes of each node and have to be added on-line during the search, which requires an appropriate model.

#### 4.3. Risk

Primary requirement of the path planning is to generate collision free paths. However, it is good to include the probability of success as well, if the method is going to be used in real life situations. Unexpected robot actions or non-deterministic environment can lead to an undesirable collision or to getting stuck, if some risk criteria are neglected. The robot may hit the obstacle if it moves too close because of unexpected disturbances in the environment or a simple slip.

This criterion is usually handled by controllers that are not directly connected with the global path planning, but some experiments of incorporating the risk function into the search algorithm cost functions have also been conducted. Risk cost methods are often used for navigation of the vulnerable vehicles that are very sensitive to any disturbance, like UAVs (De Filippis, Guglieri and Quagliotti, 2011; Dogan, 2003) or holonomic vessels (Greytak and Hover, 2009). In the cost function, risk is included along with other criteria in the current path cost and is neglected in the heuristic, which makes it admissible.

#### 4.4. Explicit energy consumption

The above methods are justified when energy considerations are unimportant, or can be expressed through other measures (like path length). Robots usually

operate using energy stored in the batteries of limited capacity, which also have other limitations, like available voltage or current. This situation encourages development of more efficient energy consumption strategies to lengthen the operation time of, for example, exploration robots, mechanisms like manipulators (Kato, Ichiyama, Tamamoto and Ohkawa, 1994) or cable robotic systems (Borgstrom et al., 2008). Explicit calculation of energy is widely used for mobile robots. Ge Yang and Rubo Zhang (Yang and Zhang, 2009) proposed the Particle Swarm Optimization (PSO) method to minimize the energy cost for autonomous underwater vehicles, taking also into account strong water currents of known location and parameters. Other methods focus on the energy consumption associated with resistances to motion, like friction, terrain shape and gravity. In Zheng and Reif (2003) the terrain height is also included in calculations in the form of potential energy connected with gravity force. In Liu and Sun (2011) more optimization aspects are added in local trajectory planning, including changing curvatures and velocity. In Mei, Lu, Hu and Lee (2004) the energy is calculated based on the wheel velocities rather than friction and terrain shape.

All of the approaches presented above operate on information that is either stored in the map representation or comes from vehicle dynamics models – only weak relations between both data sources are considered. In this paper, we suggest stronger dependencies between the robot and the environment representation, both the interactions between terrain and robot tires, and the movement direction of the vehicle are taken into account.

## 5. Model of a four-wheeled mobile robot

For global path planning of 4WMR its simplified dynamics model is applied, this model being valid for small roll angles of robot body. It is assumed that the robot moves with desired constant velocity  $v \leq v_{max}$  on an even ground surface with known constant inclination  $\beta$  (which is positive when the robot moves down the slope) and known coefficients of maximum friction  $\mu$  and rolling resistance  $f_r$  between the tire and the ground. Assuming that the robot velocity is low, the influence of aerodynamic forces on its motion can be neglected. It is assumed that the robot body lateral tilt  $\alpha$  (also known as roll angle) is small, i.e. less than 5 deg.

The vehicle used for simulations in this paper is a 4WMR with front wheels driven. The model of robot dynamics is developed assuming that its motion takes place in the  $Rxz$  plane (Fig. 2). The quantities associated with the wheels of the robot are marked with subscripts  $f$  and  $b$ , respectively, for front and back wheels.

It is assumed that the robot wheels roll without slip, therefore the following relationship is satisfied:

$$v = \dot{\theta}_i r \quad \Rightarrow \quad \dot{\theta}_i = v/r, \quad (3)$$

where:  $i = \{f, b\}$ ,  $\theta_i$  – wheel rotation,  $r$  – wheel radius.



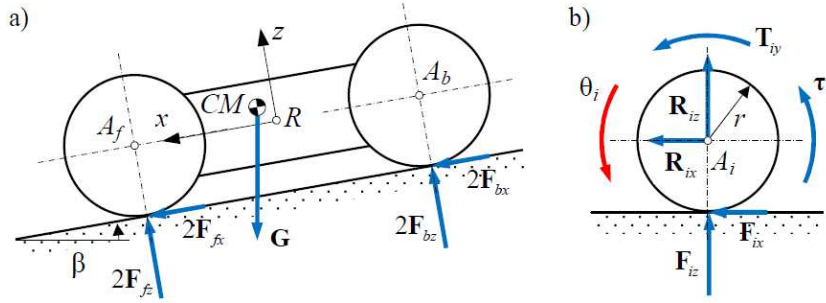


Figure 2. a) Simplified model of the robot moving on a slope, b) model of the wheel

$$(L = A_f A_b, G = m_R g, \beta = \text{const}, i = \{f, b\})$$

The assumption of rolling of robot wheels without slipping is present in the majority of publications related to modeling of the dynamics of wheeled mobile robots, the examples of such studies being Hendzel (2007), Pousti and Bodur (2008), Velazquez and Lay-Ekuakille (2011), Moosavian, Alipour and Bahramzadeh (2007), Park and Minor (2004). This simplification is justified in the case of wheeled robots having steered wheels (similarly to automotive vehicles) or caster wheels moving at low velocity and low acceleration on even and homogeneous ground surface. This is due to the fact that high value of linear velocity of robot movement leads to high value of centripetal acceleration during cornering and thus to large lateral slip, whereas high value of linear acceleration results in large longitudinal slip. Therefore, wheel slips should be taken into account in these studies, in which the exact linear velocity-time characteristic and maximum values of acceleration, as well as the shape of the motion path during cornering, are planned. In this paper, which focuses on the issue of global path planning, robot motion with a constant linear velocity between particular positions on the map is assumed. Moreover, due to relatively large distances between considered successive positions of the robot, as compared to its dimensions, the radius of cornering resulting from the change of motion direction is omitted.

Moreover, it is known from kinematics that the robot moving with a constant velocity after time  $t_m$  covers the distance of  $s$ , i.e.:

$$s = v t_m \quad \Rightarrow \quad t_m = s/v. \quad (4)$$

The dynamic equations of motion of the robot have the form (see Fig. 2a):

$$m_R \dot{v} = 2F_{fx} + 2F_{bx} + m_R g \sin(\beta) = 0, \quad (5)$$

$$2F_{fz} + 2F_{bz} - m_R g \cos(\beta) = 0, \quad (6)$$

$$2F_{bz} (L/2 + x_{CM}) - 2(F_{fx} + F_{bx}) (r + z_{CM}) - 2F_{fz} (L/2 - x_{CM}) = 0, \quad (7)$$

where:  $g$  – gravitational acceleration,  $m_R$  – robot's total mass,  $x_{CM}$ ,  $z_{CM}$  – robot's center of mass coordinates,  $L$  – distance between the front and rear axles,  $F_{fx}$ ,  $F_{bx}$ ,  $F_{fz}$ ,  $F_{bz}$  – the longitudinal ( $x$ ) and normal ( $z$ ) components of ground reaction forces for front ( $f$ ) and back ( $b$ ) wheels in accordance with Fig. 2a.

Equation (5) follows from the Newton's second law. Because of the assumption of the robot motion at constant velocity  $v = const$ , robot acceleration in the direction of  $x$  axis is equal to 0. For simplicity, the phases of the robot motion, associated with acceleration and braking, are omitted, assuming that the distances traveled by the robot during these phases are small in relation to the distances between neighboring nodes.

Equation (6) results from the equilibrium of forces in the  $z$ -direction, i.e., normal to the ground. Because there is no robot movement in this direction, the sum of projections of all forces on the  $z$  axis must be equal to 0.

Similarly, it is assumed that the robot during motion on an inclined plane (with constant inclination  $\beta$ ) does not undergo any rotation about the transverse axis ( $y$ ). Therefore, during analysis of the robot motion in the  $Rxz$  plane, one may notice that the sum of the moments resulting from all the forces with respect to any chosen point, for example the robot center of mass, is equal to 0, which is described by equation (7). It should be noted that the moments about this point result from the ground reaction forces  $F_{fx}$ ,  $F_{bx}$ ,  $F_{fz}$  and  $F_{bz}$ , i.e., forces associated with the contact of the wheels with the ground.

The relationships (5)-(7) concern only the case of the robot motion on an inclined plane with a constant angle  $\beta$ . In the model of robot dynamics the possibility of change of this angle is neglected, because only approximate representation of the terrain, on which the robot moves, is assumed for simplicity.

Dynamic equations of motion of the robot's  $i^{th}$  wheel can be written as (see Fig. 2b):

$$I_{Wy} \ddot{\theta}_i = \tau_i - F_{ix} r + T_{iy} = 0, \quad (8)$$

where:  $I_{wy}$  – wheel moment of inertia about its spin axis,  $\tau_i$  – driving torque ( $\tau_b = 0$ , because only the front wheels are driven),  $T_{iy} = F_{iz} f_r r$  – rolling resistance torque,  $i = \{f, b\}$ .

The solution to the system of equations (5)–(8) is as follows:

$$\tau_f = m_R g r (f_r c_\beta - s_\beta) / 2, \quad (9)$$

$$F_{fx} = -m_R g (L s_\beta + f_r (-l_f c_\beta + h s_\beta)) / (2L), \quad (10)$$

$$F_{bx} = -m_R g f_r (l_f c_\beta - h s_\beta) / (2L), \quad (11)$$

$$F_{fz} = m_R g (l_b c_\beta + h s_\beta) / (2L), \quad F_{bz} = m_R g (l_f c_\beta - h s_\beta) / (2L), \quad (12)$$

where:  $s_\beta = \sin(\beta)$ ,  $c_\beta = \cos(\beta)$ ,  $l_f = L/2 + x_{CM}$ ,  $l_b = L/2 - x_{CM}$ ,  $h = r + z_{CM}$ ,  $l_f$ ,  $l_b$  – distances from the center of mass of the robot to the axles of front and rear wheels, respectively, measured in the direction of the  $x$  axis,  $h$  – distance

from the center of mass of the robot to the ground, measured in the direction of the  $z$  axis (according to Fig. 2a).

In addition, to make the desired robot motion possible, the longitudinal and normal reaction forces must satisfy the relationships:

$$F_{iz} > 0, \quad |F_{ix}| \leq \mu F_{iz}, \quad (13)$$

where the second dependence results from the Coulomb model of friction.

The model of robot motors (that drive the front wheels) is described by the following dependences, which are typically used for modeling DC motors (Hong Jun and Byung Kook, 2010):

$$\tau_f = \eta_d n_d k_m i_f \quad \Rightarrow \quad i_f = \tau_f / (\eta_d n_d k_m), \quad (14)$$

$$u_f = k_e n_d \dot{\theta}_f + R_d i_f, \quad (15)$$

where:  $n_d$  – gear ratio,  $\eta_d$  – efficiency factor of the gear transmission,  $k_m$  – motor torque coefficient,  $i_f$  – rotor current,  $u_f$  – motor voltage input,  $k_e$  – electromotive force constant,  $R_d$  – rotor resistance.

Moreover, due to the motor limitations regarding electric power  $p_{max}$ , voltage  $u_{max}$  and torque  $\tau_{max}$ , the following dependences must be fulfilled:

$$u_f i_f \leq p_{max}, \quad |u_f| \leq u_{max}, \quad |\tau_f| \leq \tau_{max}. \quad (16)$$

Electrical energy, needed to achieve the assumed movement of the robot, equals:

$$E = \int_0^{t_m} (2 u_f i_f + p) dt = (2 u_f i_f + p) t_m, \quad (17)$$

where:  $p = const$  – electrical power needed to supply robot devices, regardless of whether the robot is moving or not, and  $2 u_f i_f = const$ , which follows from the introduced robot model and assumed constant velocity ( $v = const$ ).

It is also assumed that the robot cannot recover the energy lost through braking, e.g., during down the slope motion.

## 6. The energy efficient path planning approach

### 6.1. Terrain representation

The real terrain representation, usually a 2D discrete model, should be accurate enough to preserve the sense of path planning. The size of each grid cell of the decomposed terrain map should be small enough to avoid terrain information loss and misinterpretation of the size of the actual obstacles.

However, in this paper the accuracy of the representation is not the main goal and some terrain simplifications are acceptable, and, in this connection also, the accurate path shape is not investigated. The map of the environment is decomposed into cells and is represented as a grid. Each grid element represents a discrete part of the working space, which contains information about terrain

height and type. Tire-ground interface for every terrain type is characterized by friction and rolling resistance coefficients. The most common square-shaped grid type is used. The number of cells depends on map size, and dimensions of each cell are larger than dimensions of the robot. This assumption guarantees – without extra algorithmic conditions – that every time the path is found, the robot physically never interacts with an obstacle. The side of each cell equal to 2 m was chosen.

## 6.2. Partial energies

While travelling from one place to another, the robot is crossing two different grid nodes with constant linear velocity, therefore the properties of both cells have to be considered. The robot can move from each node to one of its 8 neighboring nodes along the straight line connecting their centers. Every partial distance  $s_i = n_{i-1}n_i$  consists of one half the distance traveled within the node  $n_{i-1}$  and the other half, within the node  $n_i$ . For a partial movement from node  $n_{i-1}$  to  $n_i$ , the energy cost for the path planning algorithm is calculated as the sum of two separately calculated energies, as shown in Fig. 3, where  $E_{i-1}(n_{i-1}, n_i)$  and  $E_i(n_{i-1}, n_i)$  (e.g.  $i-1 = c$  and  $i = b$  for diagonal crossing or  $i = d$  for taxicab geometry crossing) are energies needed to travel within the boundary of, respectively, nodes  $n_{i-1}$  and  $n_i$ .

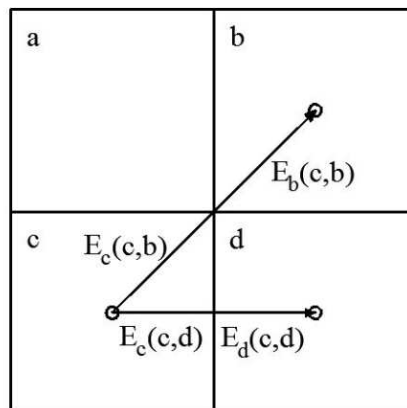


Figure 3. Partial energy costs of travel during taxicab geometry and diagonal crossing

Assuming constant velocity, the travel time for both halves of the path between nodes is the same. Situation is analogous for diagonal movement (see Fig. 3).

### 6.3. Cost function

In the following considerations, the duration of movement along the whole path is less important than the energy consumed. The energy efficient planning is the most suitable for exploration robots, because they can explore more terrain given the same amount of energy.

For the proposed 4WMR, the energy consumption will be calculated based on motor speeds (assumed constant), electric current and voltage, including all other factors like friction, gravity, and terrain height. The battery discharge curve as well as input voltage, current, power, driving torque, and wheel rotational velocity constraints are included in the calculation. The cost  $g(n_i)$ , including terrain model, described in subsection *A* is assumed as follows:

$$g(n_i) = g(n_{i-1}) + E(n_{i-1}, n_i); \quad g(n_0) = 0; \quad i = 1, 2, 3, \dots, K, \quad (18)$$

where:

$$E(n_{i-1}, n_i) = E_{i-1}(n_{i-1}, n_i) + E_i(n_{i-1}, n_i). \quad (19)$$

Due to terrain decomposition into cells (described in Section 6.1), the partial energy  $E(n_{i-1}, n_i)$ , consumed by the robot traveling the distance  $s_i = n_{i-1}n_i$ , has to be divided into two parts, associated with terrain data from nodes  $n_{i-1}$  and  $n_i$ . Energy consumption is calculated based on the robot model. The distance between two nodes is always divided into half. Therefore, calculation of time is based on the desired constant velocity and the length of the half of the partial distance of the decomposed map.

To keep the algorithm admissible, the heuristic part  $h(n_i)$  must be non-negative and thus it consists only of the value of energy consumption of robot electrical devices, i.e.:

$$h(n_i) = p \frac{S_i}{v}, \quad (20)$$

where  $S_i$  is the Euclidean distance from node  $n_i$  to the destination.

It should be noted that the real energy consumption of the robot will be higher than the one computed by the algorithm, because of simplifications in the energy cost function. The algorithm of cost computation does not include:

- acceleration at the beginning and braking at the end of the path,
- velocity changes during path execution,
- complexity of real terrain (simplified terrain representation is used),
- additional energy cost required to make turns (which is especially important in the case of skid-steered mobile robots).

### 6.4. Limitations

Limitations of robot roll and pitch angles, which result from the constraints (13) on the ground reaction forces, are taken into account. Both restrictions have to

be respected during every partial robot movement, i.e.:

$$\alpha_{\max} \geq \alpha \geq \alpha_{\min}, \beta_{\max} \geq \beta \geq \beta_{\min}. \quad (21)$$

For a given node, the slope is calculated based on properties of surrounding nodes. The energy cost depends on robot pitch angle. The robot cannot move on too steep terrain, so the pitch angle (Fig. 4a) must be calculated every time robot travels from node to node.

Robot pitch angle during the movement between starting and ending nodes (respectively  $n_{i-1}$  and  $n_i$ ) is calculated based on their heights and distance between them:

$$\beta = -\arctan((h_E - h_S)/l), \quad (22)$$

where:  $h_S, h_E$  – heights of starting and ending nodes, respectively,  $l$  – horizontal distance between those nodes.

The horizontal distance between nodes equals  $l = 2$  m during taxicab geometry crossing and  $l = 2\sqrt{2}m$  in case of diagonal movement.

Robot roll angle (Fig. 4b) is calculated based on the heights of nodes, which lie on the left- and right-hand side of the robot direction of movement (perpendicularly to the path):

$$\alpha = \arctan((h_L - h_R)/w), \quad (23)$$

where:  $h_L, h_R$  – heights of nodes situated on the left- and right-hand sides,  $w$  – horizontal distance between neighboring nodes, i.e., from the left to the right one.

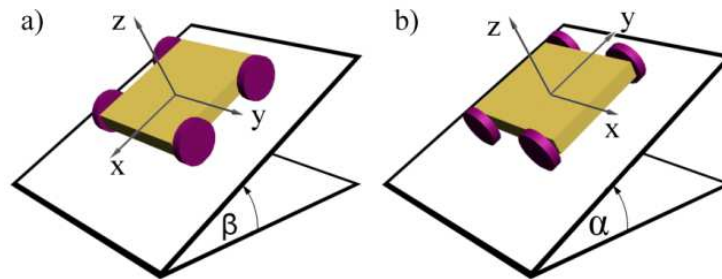


Figure 4. a) Robot pitch angle, b) robot roll angle

During taxicab geometry crossing, shown in Fig. 5a, the robot roll angle, e.g., between nodes  $d$  and  $e$ , is taken from the lateral slope, that is, calculated based on the surrounding heights  $h_{ab}$  and  $h_{gh}$  from corresponding nodes to the left and to the right of the robot. In that case  $w = 4$  m, and  $h_{ab}, h_{gh}$  are average heights from nodes  $a, b$  and  $g, h$ , respectively. In case of diagonal movement (Fig. 5b), the roll angle is directly calculated from two nodes that are perpendicular

to the path. In the case shown in Fig. 5b,  $w = 2\sqrt{2}m$  and the heights of nodes  $d$  and  $h$  are taken for the lateral slope angle calculation.

Distance between two nodes, after taking into account the terrain slope  $\beta$ , is given by:

$$s = l / \cos(\beta). \quad (24)$$

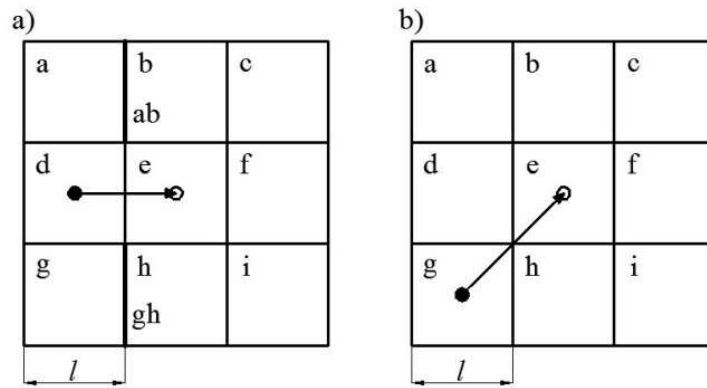


Figure 5. a) Taxicab geometry crossing b) diagonal crossing

Every node of the grid contains information about terrain type. The terrain types used in simulation are shown in Table 1, based on data from Wong (2001). The value of  $f_r$  for ice was not found in the literature, but estimated by the authors.

Table 1. Coefficients characterising interactions between robot tires and particular terrain types, Wong (2001)

Terrain type	Known coefficients	
	friction $\mu$	rolling resistance $f_r$
Concrete / asphalt	0.8	0.015
Unpaved road	0.68	0.05
Rolled gravel	0.6	0.02
Ice	0.1	0.01

It is assumed that the robot mass center is located at point  $R$  (see Fig. 2a), that is, relatively low. Regarding this, the robot will slip on ground surface rather than flip over. Therefore, the maximum roll angle for a robot (Fig. 4b)

should take into account the worst case, i.e., moving on an ice surface. In this case it equals:

$$\alpha_{\max} = \arctan(\mu) = 5.7 \text{ deg}, \quad \alpha_{\min} = -\arctan(\mu) = -5.7 \text{ deg}. \quad (25)$$

Determination of the pitch angle constraints is much more complicated, because it depends on coefficients of friction and rolling resistance, as well as position of robot mass centre. The exact, general solution, resulting from the model of robot dynamics (see Section 5 for more details), is in this case complex.

The obtained allowable ranges of roll and pitch angles, resulting from the model of dynamics of the robot, for various terrain types are shown in Table 2.

Table 2. Allowable ranges of roll and pitch angles for various terrain types, from the robot dynamics model

Terrain type	Range	
	Roll angle [deg]	Pitch angle [deg]
Concrete / asphalt	(-38.7, +38.7)	(-18.1, +26.7)
Unpaved road	(-34.2, +34.2)	(-15.0, +23.3)
Rolled gravel	(-31.0, +31.0)	(-14.1, +19.8)
Ice	(-5.7, +5.7)	(-2.5, +3.2)

All variables, like the required input voltage and current, are calculated at each iteration step, so that the battery discharge curve and other limitations can be taken into account. The required input voltage for every motor at every partial calculation must fulfill the nominal battery voltage and capacity constraints. Battery capacity  $c(n_i)$ , required to execute a potential path from the start to node  $n_i$ , is calculated based on total current flow during traveling time. This consists of the sum of partial products  $i_j t_j$  for every path step, i.e.:

$$c(n_i) = \sum_{j=1}^i (i_j + i_{j-1}) t_j / 2, \quad c(n_0) = 0. \quad (26)$$

Every time the algorithm visits a node, the required and available capacities are checked against the following condition:

$$c(n_i) \leq c_a \quad (27)$$

where:  $c_a$  – battery available capacity,  $c(n_i)$  – required capacity.

## 7. Energy consumption

Figure 6 shows the calculated values of energies required for the motion of the robot on various types of terrain for various pitch angles, for constant desired velocity of the robot and cell size. These calculations have been carried out for



velocity  $v = 1$  m/s, cell size  $s = 2$  m, and electrical power consumption of robot on-board devices  $p = 1$  W. All limitations and requirements described earlier are included. Energy recovery is omitted, and, consequently, any energy value required for the robot motion lower than 0 J (calculated on the basis of the robot model) in the path planning algorithm is treated as 0 J. Moreover, electrical power needed to supply the robot devices has been taken into account. This implies that cost is always non-negative, which is required for proper working of the A\* algorithm, and its minimum value equals to  $E_{min} = pt_m$ .

The highest values of the required energy are for unpaved road because it has the highest value of rolling resistance coefficient. The narrowest range of pitch angles is for the ice surface, because it has the lowest value of maximum friction coefficient (see Table 2).

If at least one of the conditions described previously is not satisfied, the node is treated as unavailable and the cost associated with this node,  $E(n_{i-1}, n_i)$ , is set to a very large value (higher than battery capacity), deemed too expensive from the point of view of the algorithm.

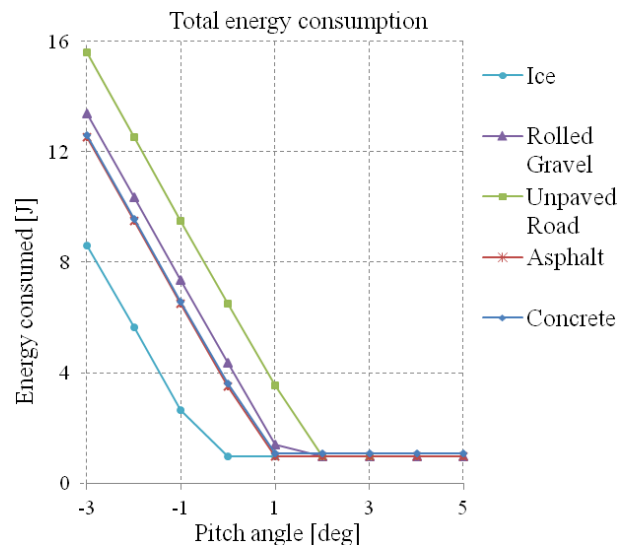


Figure 6. Total energy consumption for different pitch angles

## 8. Simulation results and discussion

Several simulations have been conducted to highlight the differences between energy consumption of the standard shortest path approach, where the cost function is represented as path length, and the energy efficient planning method, proposed in this paper, where cost is connected with electrical energy. The maps of 1600 m<sup>2</sup> areas of field and urban environments were decomposed into 20x20

equal-sized square-shaped elements. Two different paths have been found for each simulation, as shown in Fig. 7: the one represented with white dots – the shortest one, and another, represented with black dots – the energy efficient one.

The following robot parameters were assumed for all simulations:

- dimensions:  $L = 0.35$  m,  $r = 0.085$  m (see Fig. 2),
- mass parameters:  $m_R = 13.73$  kg,  $x_{CM} = 0$  m,  $z_{CM} = 0$  m,
- parameters of drive units:  $L_d = 0.0000823$  H,  $R_d = 0.317$   $\Omega$ ,  $k_e = 0.0301$  Vs/rad,  $k_m = 0.0302$  Nm/A,  $n_d = 34.67$ ,  $\eta_d = 0.8$ ,
- parameters of battery:  $c_a = 4.6$  Ah,  $u_a = 8 \times 3.7$  V (nominal voltage of the 8-cell battery).

Differences between energy consumption of the two approaches are shown in the series of experiments for various velocities  $v$  and electrical power consumption of robot devices  $p$ , as shown in Figs. 8–11. The shortest path approach yields a shorter path than the energy efficient one, but it is more energy consuming. In application scenarios, when travel time is less important than energy consumption, the method proposed in this paper performs better.

Energy costs of paths determined using different approaches, for various constant velocities  $v$  and power consumption of robot devices  $p = 1$  W, and for both maps, are shown in Figs. 8 and 9. Higher speed values decrease the total time required for the robot to travel from the start to destination, so the energy cost for a path becomes lower with increasing velocity in case of the same paths.

The energy-based method minimizes the energy used by the robot by means of minimizing the energy equation (17). An important role is played by the electrical power  $p$  needed to supply the electrical devices of the robot. If the constant part of that equation ( $p$ ) is big enough, then the second product ( $u \cdot i$ ) may become less important, in which case the energy efficient planning problem turns into the problem of finding the minimum of the  $p\Delta t$  product. Because  $p$  is constant (independent of time), the time  $t$  becomes the only variable that matters in minimizing the equation. Then, the energy efficient problem yields a solution that is similar to the solution of the shortest distance approach method, where the time is strictly connected with distance. This can be observed by comparing the energy costs of the required start-goal path for various  $p$  as shown in Figs. 10 and 11. Path length changes very significantly between certain values of  $p$  ( $p = 2$  W and  $p = 3$  W in Figs. 10 and 11). This shows that the energy efficient method becomes the shortest distance problem for sufficiently large values of  $p$ .

For maps shown in Fig.7, energy consumption for energy efficient path planning is lower than for the shortest path planning method. Energy savings grow for maps with more diverse terrain. However, for the case of the field environment and the start and destination positions selected as shown in Fig.12, it is still possible to prove that small extension of distance (approximately 1.5%) can lead to almost 30% of energy savings as shown in Fig.13.

In order to shorten the calculation time of the optimal path, the admissible heuristic containing the electrical power consumption of electrical devices of the

robot is taken into account, as described earlier. This function always leads to the optimal path, but it does not always perform its task of estimating the path energy cost in the best possible way, and so the algorithm does not always provide the most efficient path. It is likely that there exist other algorithms or heuristics, which guarantee optimal path with fewer nodes expanded during the search process.

## 9. Summary and future works

Experiments with two different approaches, the shortest distance and the energy efficient method proposed in this paper, show that:

- Energy savings are clear even for small maps;
- The energy efficient approach becomes the shortest distance approach in case when the constant electric power consumption of robot devices  $p$  rises significantly as compared to the electrical power consumed by motors;
- Some other form of the heuristic is necessary to achieve the optimum algorithm efficiency.

The energy efficient planning method, presented in this paper, always gives the energy efficient path, but the algorithm is not always optimally efficient. The better heuristic should be elaborated, or an efficient way of choosing the right one according to the map must be developed.

A more accurate terrain shape, fine cell map decomposition and robot representation may be implemented, which will take into account robot dimensions and more diverse features of terrain.

Further research may also include:

- Enhancement of the model of robot dynamics by taking into account the possibility of robot turning, which will influence the calculation of energy consumption;
- Optimization of the shape of the path – for example – of the turning radii;
- Taking into consideration the variable velocity of robot motion.

## 10. Acknowledgment

The work has been realized as a part of the project entitled “Dynamics modeling of a four-wheeled mobile robot and tracking control of its motion with limitation of wheel slip”. The project is financed from the means of National Science Centre of Poland granted on the basis of decision number DEC-2011/03/B/ST7/02532.

We also gratefully acknowledge the editorial assistance as well as important comments and suggestions provided by Mr. Przemysław Dąbek of the PIAP Fundamental Research Team.

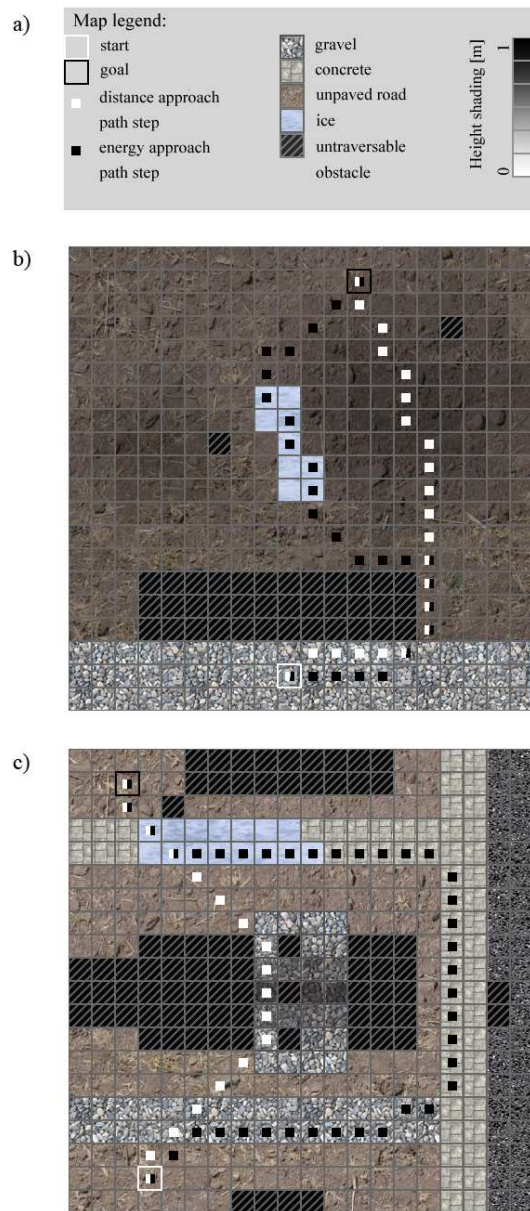


Figure 7. a) Map legend; paths found with the shortest path approach (white dots) and the energy efficient approach (black dots) for the maps of: b) field environment, c) urban environment

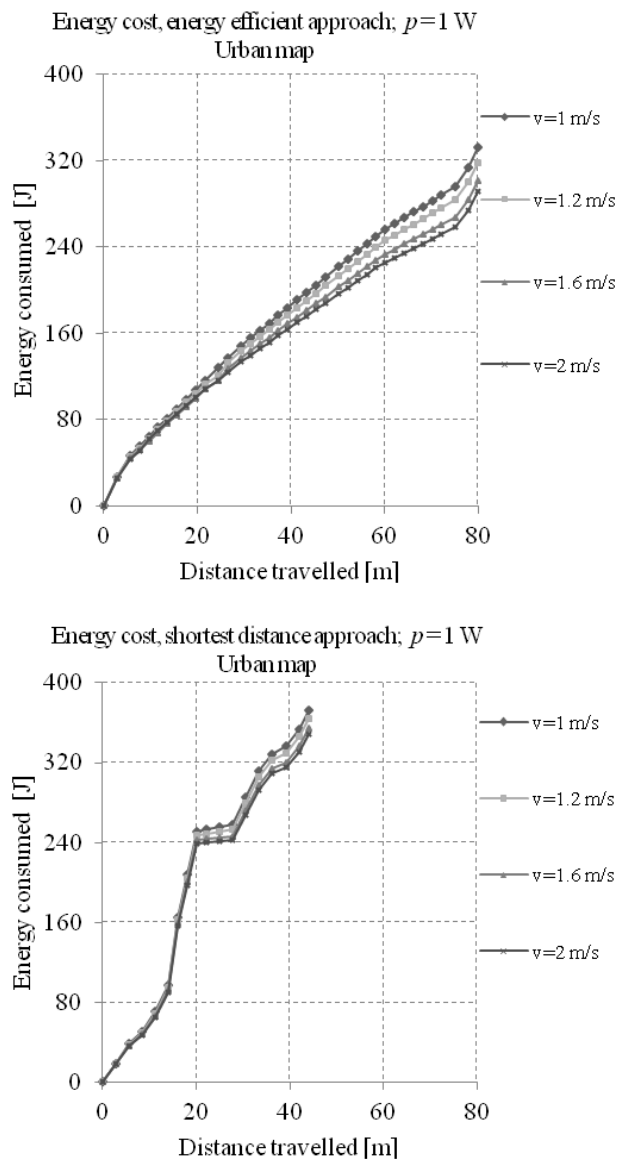


Figure 8. Energy costs for various constant velocities on the urban map using both approaches

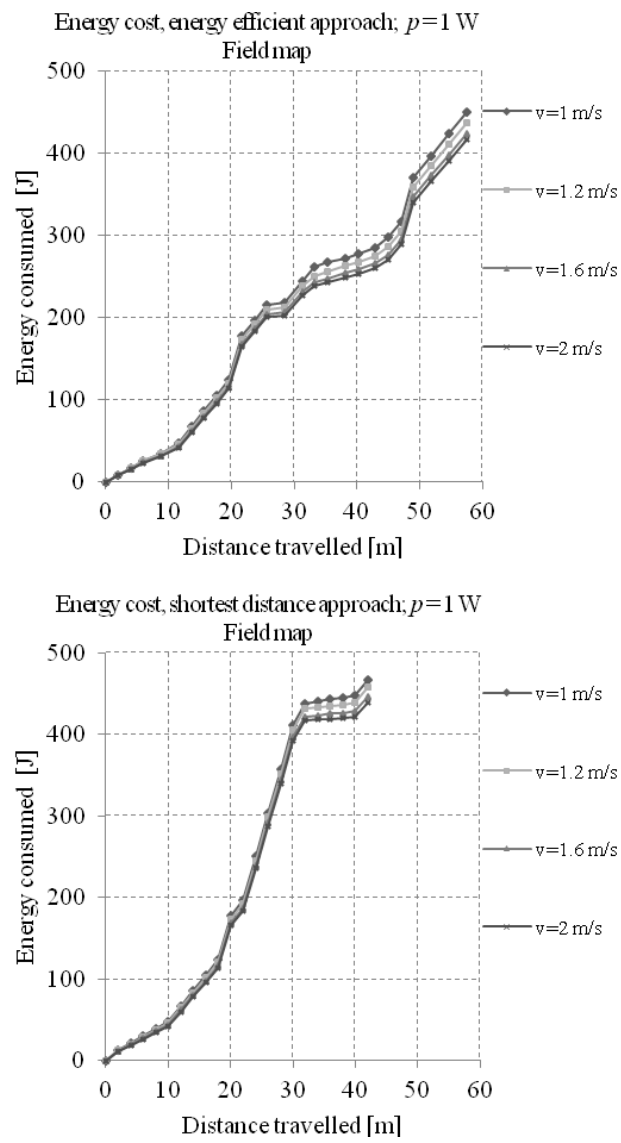


Figure 9. Energy costs for various constant velocities on the field map using both approaches

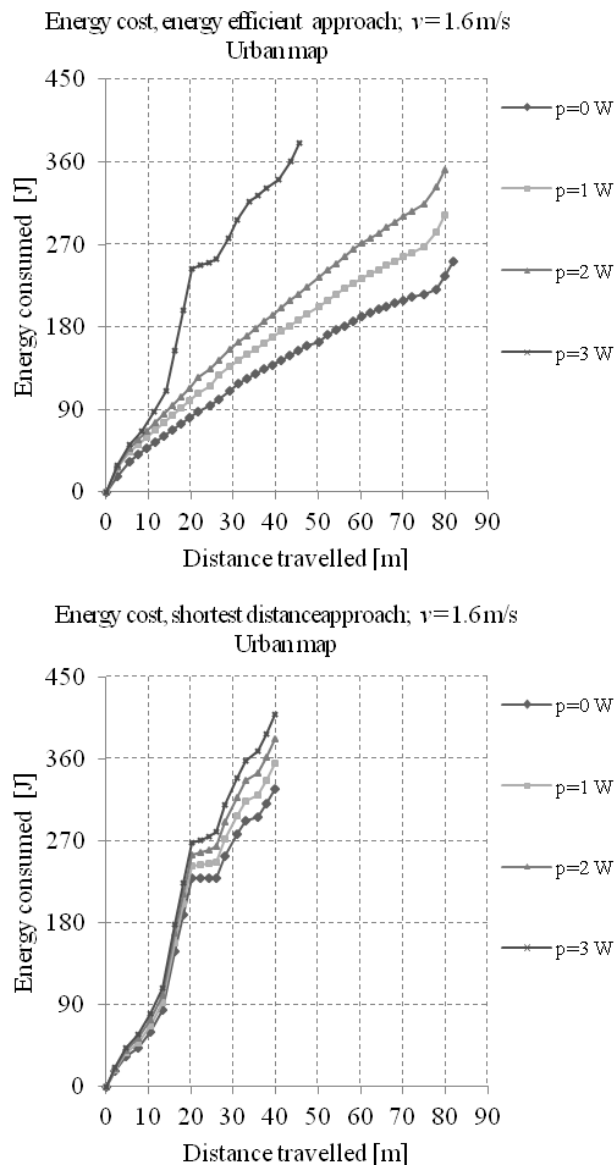


Figure 10. Energy costs for various constant  $p$  on the urban map using different approaches

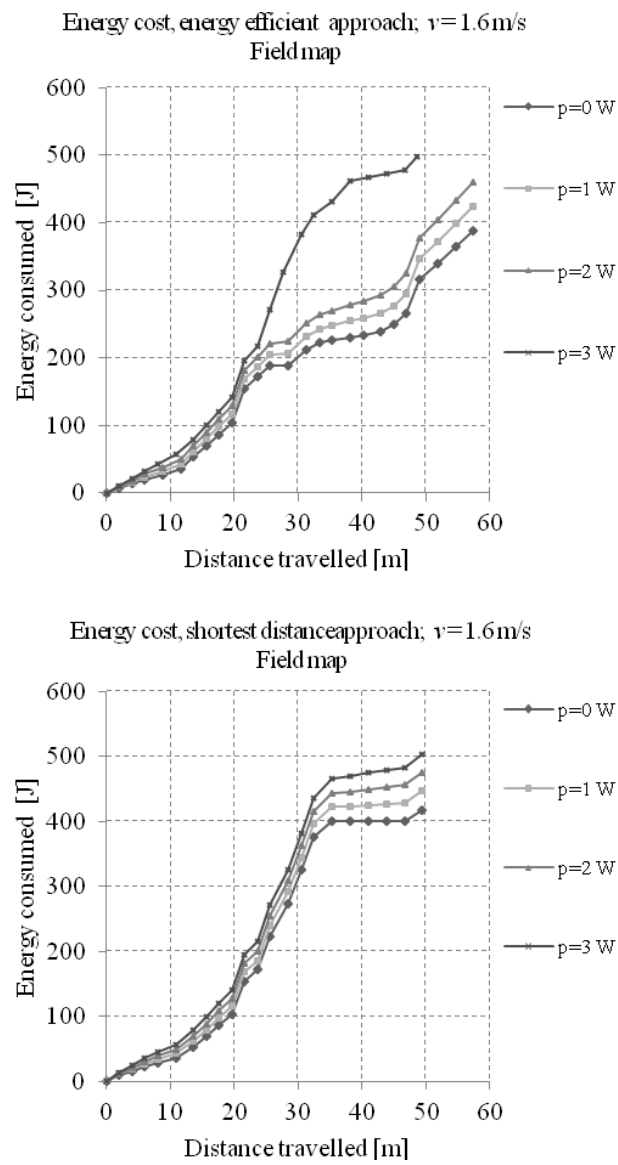


Figure 11. Energy costs for various constant  $p$  on the field map using different approaches



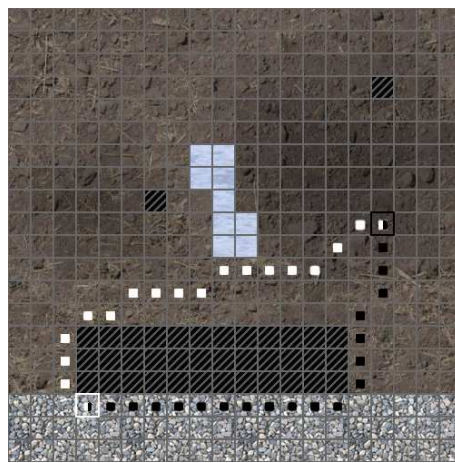


Figure 12. Example of a situation with similar path lengths, but large difference in robot energy consumption for the paths

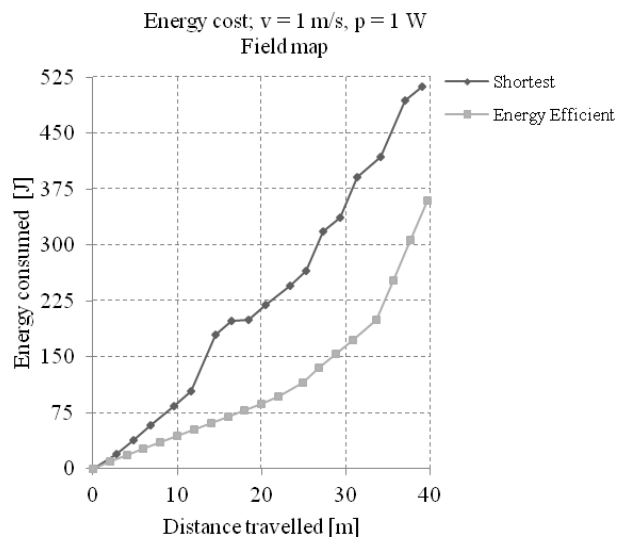


Figure 13. Situation in which in the field map, the difference of energy consumed over similar travel distance for two different approaches can reach almost 30%

## References

- BIGAJ, P. (2012) *Global Path Planning for Mobile Robots*. Oficyna wydawnicza PIAP, Warszawa.
- BORGSTROM, P., SINGH, A., JORDAN, B., SUKHATME, G., BATALIN, M., KAISER, W. (2008) Energy based path planning for a novel cabled robotic system. *IEEE/RSJ International Conference on Intelligent Robots and Systems*. IEEE , 1745-1751.
- DE FILIPPIS, L., GUGLIERI, G., QUAGLIOTTI, F. (2011) A Minimum Risk Approach for Path Planning of UAVs. *Journal of Intelligent & Robotic Systems*, **61**(1-4), 203-219.
- DOGAN, A. (2003) Probabilistic approach in path planning for UAVs. *2003 IEEE International Symposium on Intelligent Control*. IEEE, 608-613.
- DOLGOV, D. T., THRUN, S., MONTEMERLO, M., DIEBEL, J. (2008) Path Planning for Autonomous Driving in Unknown Environments. *Proceedings of the Eleventh International Symposium on Experimental Robotics (ISER-08)*. Springer, Berlin-Heidelberg.
- GREYTAK, M., HOVER, F. (2009) Motion Planning with an Analytic Risk Cost for Holonomic Vehicles. *Joint 48th IEEE Conference on Decision and Control and 28th Chinese Control Conference*, Shanghai. IEEE, 5655-5660.
- HEART, P. E., NILSSON, N. J., BERTRAM, R. (1968) A Formal Basis for the Heuristic Determination of Minimum Cost Paths. *IEEE Transactions on Systems Science and Cybernetics*, **4**(2), 100-107.
- HENDZEL, Z. (2007) An adaptive critic neural network for motion control of a wheeled mobile robot. *Nonlinear Dynamics*, **50** (4), 849-855.
- HONG JUN, K., BYUNG KOOK, K. (2010) Minimum-energy trajectory planning on a tangent for battery-powered three-wheeled omni-directional mobile robots. *Control Automation and Systems (ICCAS), 2010 International Conference*, Gyeonggi-do. IEEE, 1701-1706.
- KATOH, R., ICHIYAMA, O., TAMAMOTO, T., OHKAWA, F. (1994) A real-time path planning of space manipulator saving consumed energy. *Control and Instrumentation, 1994. IECON '94, 20th International Conference on Industrial Electronics*. IEEE, 1064-1067.
- LAU, B., SPRUNK, C., BURGARD, W. (2009) Kinodynamic motion planning for mobile robots using splines. *IEEE/RSJ Int. Conf. on Intelligent Robots and Systems*, St. Louis. IEEE, 2427-2433.
- LIU, S., SUN, D. (2011) Optimal Motion Planning of a Mobile Robot with Minimum Energy Consumption. *2011 IEEE/ASME International Conference on Advanced Intelligent Mechatronics*, Budapest. IEEE, 43-48.
- MCNINCH, L. C., MUSKE, K. R., ASHRAFIUON, H., PEYTON, J. C., SOLTAN, R. A. (2011) Real-time Coordinated Trajectory Planning and Obstacle Avoidance for Mobile Robots. *Journal of Automation, Mobile Robotics & Intelligent Systems*, **5**(1), 23-29.
- MEI, Y., LU, Y.-H., HU, C. Y., LEE, G. (2004) Energy-Efficient Motion

- Planning for Mobile Robots. *Proceedings of the 2004 IEEE International Conference on Robotics & Automation*, New Orleans. IEEE, 4344-4349.
- MEI, Y., LU, Y.-H., LEE, G. C., HU, Y. C. (2006) Energy-Efficient Mobile Robot Exploration. *Proceedings of the 2006 IEEE International Conference on Robotics and Automation*, Orlando. IEEE, 505-511.
- MOOSAVIAN, S., ALIPOUR, K., BAHRAMZADEH, Y. (2007) Dynamics modeling and tip-over stability of suspended wheeled mobile robots with multiple arms. *Intelligent Robots and Systems, 2007. IROS 2007. IEEE/RSJ International Conference*, San Diego. IEEE, 1210-1215.
- PARK, S., MINOR, M. (2004) Modeling and dynamic control of compliant framed wheeled modular mobile robots. *Proceedings. ICRA '04. 2004 IEEE International Conference, 4*. IEEE, 3937 - 3943.
- POUSTI, A., BODUR, M. (2008) Kinematics and Dynamics of a Wheeled Mobile Inverted Pendulum. *2008 International Conference on Computational Intelligence for Modelling Control & Automation*, Vienna. IEEE, 409-413.
- RUSSELL, S., NORVIG, P. (1995) *Artificial Intelligence - A Modern Approach* (3rd ed.). Pearson Education, New Jersey.
- STENTZ, A. (1995) The focussed D\* algorithm for real time replanning. *Proceedings of the International Joint Conference of Artificial Intelligence*. San Francisco. Morgan Kaufman Publishers, 1652-1659.
- STENTZ, A., FERGUSON, D. (2005) An interpolation-based path planner and replanner. *Proceedings of the Int. Symp. on Robotics Research (ISRR)*. Springer, Berlin-Heidelberg, 1-10.
- SZULCZYŃSKI, P., PAZDERSKI, D., KOZŁOWSKI, K. (2011) Real-Time Obstacle Avoidance Using Harmonic Potential Functions. *Journal of Automation, Mobile Robotics & Intelligent Systems*, **5**(3), 59-66.
- VELAZQUEZ, R., LAY-EKUAKILLE, A. (2011) A review of models and structures for wheeled mobile robots: Four case studies. *Advanced Robotics (ICAR), 2011 15th International Conference*, Tallinn. IEEE, 524-529.
- WINTER, S. (2002) Modeling Costs of Turns in Route Planning. *GeoInformatica*, **6**(4), 345-361.
- WONG, J. Y. (2001) *Theory of Ground Vehicles* (3rd ed.). Wiley-Interscience.
- YANG, G., ZHANG, R. (2009) Path Planning of AUV in Turbulent Ocean Environments Used Adapted Inertia-weight PSO. *Fifth International Conference on Natural Computation*. IEEE, 299-302.
- YU, Y., WANG, H., YUAN, Q. (2011) Application of Dijkstra algorithm in robot path-planning. *Second International Conference on Mechanic Automation and Control Engineering (MACE)*. IEEE, 1067-1069.
- ZHENG, S., REIF, J. (2003) On Energy-minimizing Paths on Terrains for a Mobile Robot. *ICRA '03. IEEE International Conference on Robotics and Automation, 3*. IEEE, 3782-3788.